

# Composition of Oxide Compounds Supported on Metal Meshes when Synthesizing Catalysts for the Oxidation of Hydrocarbons

K. I. Shefer<sup>a, b, \*</sup>, E. M. Moroz<sup>a</sup>, V. N. Rogozhnikov<sup>a, c</sup>, and A. V. Porsin<sup>a, c</sup>

<sup>a</sup>*Boreshkov Institute of Catalysis, Siberian Branch, Russian Academy of Sciences, Novosibirsk, 630090 Russia*

<sup>b</sup>*Novosibirsk State University, Novosibirsk-90, 630090 Russia*

<sup>c</sup>*OOO Unicat, Novosibirsk, 630090 Russia*

\**e-mail: shefer@catalysis.ru*

**Abstract**—Samples of a woven mesh of metal wire (fechral) with supported aluminum hydroxide compounds are studied. Aluminum hydroxide is formed in its bayerite modification. Aluminum oxides are produced during calcination:  $\eta$ -Al<sub>2</sub>O<sub>3</sub> at 600°C, and  $\theta$ -Al<sub>2</sub>O<sub>3</sub> at 900°C. Subsequent modification with silicon, cerium, lanthanum, tungsten, and calcination at the same temperature results in the formation of their oxides. Interaction between alumina and tungsten at 600°C, and alumina and lanthanum at 900°C, are observed.

DOI: 10.3103/S1062873816110265

## INTRODUCTION

Alumina has all the qualities of an effective carrier, which is why it is used to obtain more complex carriers for catalyst synthesis [1–4]. In this work, aluminum hydroxide compounds were deposited on a mesh made of metal wire and modified with silicon, cerium, lanthanum, and tungsten in order to produce a catalyst for the oxidation of hydrocarbons. The aim of this work was to study the phase composition of the compounds that formed on the surface of the wire.

## EXPERIMENTAL

Two series of samples were examined. In the first, the wires were covered with aluminum hydroxide, and next with the appropriate precursors containing modifier elements. The samples were then calcined at 600°C. In the second series, wire samples coated with aluminum hydroxide were preliminarily calcined at 600°C before applying the precursor. These samples were also calcined at 900°C. The samples that contained tungsten were destroyed at this temperature.

Our woven mesh of Kh23Yu5T grade fechral wire of (ZAO Soyuznikhrom) was mainly composed of metallic iron, chromium, aluminum, and (in descending order) silicon, manganese, titanium, nickel, carbon, phosphorus, and sulfur. There are works on the depositing aluminum oxide on FeCrAl alloy using the sol–gel technique [5–9]. In this work, we used the Bayer process [1], adapted for the crystallization of aluminum hydroxide on the surface of a metal mesh, for deposition. Modifiers were deposited via incipient wetness impregnation. Sodium silicate was used for modification with silicon; with cerium and lantha-

num, corresponding nitrates were used; and ammonium metatungstate was used with tungsten.

Diffraction patterns were obtained using copper radiation  $\text{CuK}\alpha$  ( $\lambda = 1.5418 \text{ \AA}$ ). Measurements were made with a Thermo techno ARL X'TRA instrument. The diffraction patterns were scanned in the angular range of  $10^\circ$ – $75^\circ$  (for  $2\theta$ ), with increments of  $0.1^\circ$  and dwelling times of 10 seconds. The theoretical diffraction patterns were taken from the PDF [10] and ICSD [11] data bases. The specific surfaces of the samples were measured via nitrogen adsorption at 77 K using an ASAP-2400 device (Micrometrics, United States).

The amount of the component applied to the grid was determined from the change in the weight of the sample before and after application. The amount of aluminum oxide was 5.7 wt % of the grid weight; the amount of the modifying component (calculated with respect to its oxide) was 3 wt % of the alumina weight for the cerium and lanthanum oxides, and 5 wt % for the silicon and tungsten oxides.

Diffraction peaks belonging to an alloy of iron and chromium were observed in the diffraction pattern of the initial metal meshes (Fig. 1a). These metals have the same structural type of unit cell and the same symmetry space group, and they are the main components of the wire. The sample contained  $\alpha$ -Al<sub>2</sub>O<sub>3</sub> phase with increased unit cell parameters, indicating the dissolution of some iron and chromium ions in it. There are also peaks that belong to a solid solution of iron and chromium oxides. These oxides are often mixed because their crystallographic parameters are similar.

When aluminum hydroxide was applied to the wire, its phase formed as bayerite, the usual product of the

Bayer process (Fig. 1b). In addition, peaks that belong to the phase of the iron–chromium alloy and the solid solution of their oxides were observed. The  $\alpha$ - $\text{Al}_2\text{O}_3$  phase and the hydroxide phase in boehmite form were not found in the sample. The  $\alpha$ - $\text{Al}_2\text{O}_3$  phase initially observed on the surface of the initial wire was evidently part of the structure of the solid solution based on iron and chromium oxides. It could also have been screened by a layer of aluminum hydroxide.

After calcination at 600°C, aluminum hydroxide assumes the metastable form of  $\eta$ - $\text{Al}_2\text{O}_3$  oxide (Fig. 1c), as in [12, 13]. It has the 2 : 3 ratio of the heights of the 3.1.1 and 2.2.2 peaks that is characteristic of this oxide. The cell parameters of the oxide (Table 1) also agree with the data bases on  $\eta$ - $\text{Al}_2\text{O}_3$ .

The diffractograms of the samples modified by silicon contained the wide peak at 28.7° (2 $\theta$ ) that corresponds to amorphous silicon oxide. The samples modified with cerium contained the  $\text{CeO}_2$  phase. The size of the coherent scattering region (CSR) of the cerium oxide applied to the alumina is  $D_{111} = 45 \text{ \AA}$ . When applied to aluminum hydroxide, we observe a bimodal particle size distribution, as is apparent from the shape of the diffraction peak; the sizes of the CSRs of  $\text{CeO}_2$  are  $D_{111} = 25 \text{ \AA}$  and 105  $\text{ \AA}$ . The broad peak at 29° (2 $\theta$ ) in the diffractograms of the samples modified with lanthanum could be due to the most intense peaks of lanthanum oxide  $\text{La}_2\text{O}_3$ . The peaks of  $\text{WO}_3$  and a peak at 28.7° (2 $\theta$ ), which can be attributed to the mixed oxide  $\text{AlWO}_4$ , are seen in the diffraction patterns of samples containing tungsten. The formation of such compounds is possible because ionic radii of  $\text{W}^{3+}$  and  $\text{Al}^{3+}$  are similar: 0.65 and 0.57  $\text{ \AA}$ , respectively [14]. The sizes of the CSRs of oxides of silicon, lanthanum, and tungsten aluminate are less than 20  $\text{ \AA}$ . These samples contain  $\eta$ - $\text{Al}_2\text{O}_3$ , iron–chromium alloy, and traces of a solid solution of iron and chromium oxides.

The CSR sizes and the carrier unit cell parameters were analyzed next (Table 1). The unit cell parameter grew during modification for all of our samples, indicating interaction between the respective ions and the carrier and the distribution of ions with ionic radii larger than that of aluminum throughout the alumina structure. The CSRs of the modifier compounds for the series of samples in which the modifier was applied to aluminum hydroxide are smaller than for the series of samples with alumina, and the specific surface area is larger.

$\theta$ - $\text{Al}_2\text{O}_3$  with a CSR of about 90  $\text{ \AA}$  is formed during the calcining of low temperature oxide  $\eta$ - $\text{Al}_2\text{O}_3$  at 900°C (Fig. 1d). This modification of alumina is generally formed via the thermal decomposition of bayerite in the temperature range of ~850–1200°C [12, 13]. In addition, peaks that belong to iron–chromium alloy and a mixed oxide of iron and chromium are observed in the diffraction pattern. The phase composition of the modifiers in the samples that con-

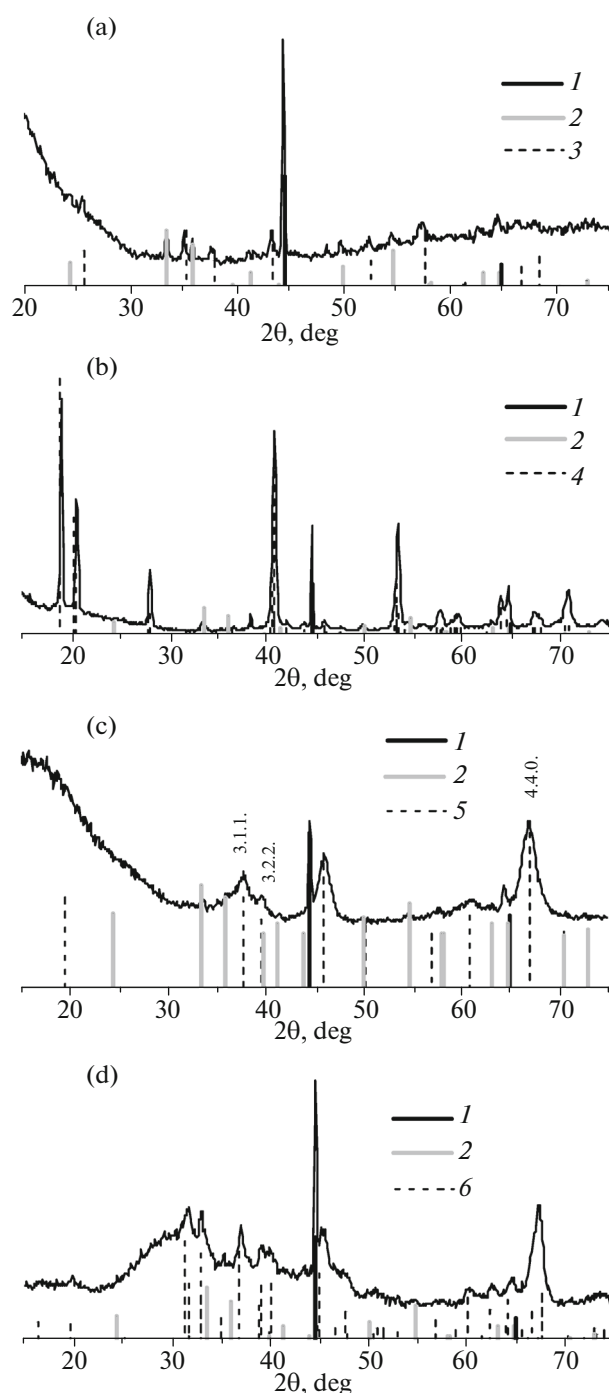


**Fig. 1.** Experimental diffraction patterns of (a) the initial metal mesh, (b) the mesh covered with alumina hydroxide, (c) the mesh covered with alumina hydroxide and calcined at 600°C, and (d) the mesh covered with alumina hydroxide and calcined at 900°C, compared to peak diagrams of (1) iron–chromium alloy, (2) iron–chromium mixed oxide, (3)  $\alpha$ - $\text{Al}_2\text{O}_3$ , (4) bayerite, (5)  $\eta$ - $\text{Al}_2\text{O}_3$ , and (6)  $\theta$ - $\text{Al}_2\text{O}_3$ .

tain oxides of silicon and cerium does not change during calcining at such temperatures. The amount of silicon oxide is reduced during calcination. The CSRs

**Table 1.** Characteristics of the samples calcined at 600°C

Sample	Sample Compound	$D_{440}(\eta\text{-Al}_2\text{O}_3)$ , Å	$a(\eta\text{-Al}_2\text{O}_3)$ , Å	$S_{\text{spec}}$ , m <sup>2</sup> /g	$V_{\text{pore}}$ , cm <sup>3</sup>
Carrier	$\eta\text{-Al}_2\text{O}_3/\text{mesh}$	65	7.914	203	0.234
First Series	Si/ $\eta\text{-Al}_2\text{O}_3/\text{mesh}$	60	7.931	184.5	0.165
	Ce/ $\eta\text{-Al}_2\text{O}_3/\text{mesh}$	65	7.928	180.4	0.172
	La/ $\eta\text{-Al}_2\text{O}_3/\text{mesh}$	65	7.918	185.5	0.170
	W/ $\eta\text{-Al}_2\text{O}_3/\text{mesh}$	65	7.927	176.8	0.200
	Si'/ $\eta\text{-Al}_2\text{O}_3/\text{mesh}$	70	7.921	125.4	0.160
Second Series	Ce'/ $\eta\text{-Al}_2\text{O}_3/\text{mesh}$	70	7.930	130.3	0.163
	La'/ $\eta\text{-Al}_2\text{O}_3/\text{mesh}$	65	7.928	148.0	0.189
	W'/ $\eta\text{-Al}_2\text{O}_3/\text{mesh}$	70	7.921	154.9	0.183

**Table 2.** Characteristics of the samples calcined at 900°C

Sample	Sample Compound	$d/n(\theta\text{-Al}_2\text{O}_3)$	$D(\theta\text{-Al}_2\text{O}_3)$ , Å	$S_{\text{spec}}$ , m <sup>2</sup> /g	$V_{\text{pore}}$ , cm <sup>3</sup>
Carrier	$\theta\text{-Al}_2\text{O}_3/\text{mesh}$	1.394	90	63.7	0.197
First Series	Si/ $\theta\text{-Al}_2\text{O}_3/\text{mesh}$	1.398	80	57.0	0.162
	Ce/ $\theta\text{-Al}_2\text{O}_3/\text{mesh}$	1.398	85	61.4	0.166
	La/ $\theta\text{-Al}_2\text{O}_3/\text{mesh}$	1.395	85	62.4	0.179
Second Series	Si'/ $\theta\text{-Al}_2\text{O}_3/\text{mesh}$	1.395	85	27.2	0.099
	Ce'/ $\theta\text{-Al}_2\text{O}_3/\text{mesh}$	1.393	85	52.4	0.184
	La'/ $\theta\text{-Al}_2\text{O}_3/\text{mesh}$	1.394	90	59.7	0.165

of cerium oxide applied to aluminum hydroxide grow to  $D_{111} = 195$  Å; when applied to the oxide, to  $D_{111} = 160$  Å. Lanthanum aluminate peaks appear in the samples that contained lanthanum oxide. In addition to these, the broad peak of lanthanum oxide is seen in the diffraction pattern of the sample with aluminum hydroxide.

The sizes of the CSR of alumina and the specific surface area during calcination of the samples at 900°C were analyzed (Table 2). Adding the modifier reduces the CSR of oxide; i.e., the surface area of the carrier should grow. The samples in which modifier was applied to aluminum hydroxide have larger specific surfaces. The specific surface area is reduced considerably if silicon is applied to aluminum oxide.

## CONCLUSIONS

We studied the phase composition of catalysts at all stages of their preparation for hydrocarbon oxidation. The difference between the phase compositions after introducing modifiers into aluminum hydroxide (in

the first series of the samples) and aluminum oxide (in the second series) was shown. When modification of alumina with silica, cerium, lanthanum, and tungsten ions, oxides or compounds of them with aluminum oxide formed on its surface. During calcining at 600°C, aluminate formed only with tungsten; during calcining at 900°C, lanthanum aluminate was formed.

## ACKNOWLEDGMENTS

Our samples were synthesized with the support of the Skolkovo Foundation and BP (project UNIHEAT). X-ray analysis was supported by base budget financing (government contract), project V.44.1.17.

## REFERENCES

1. Stiles, A.B., *Catalyst Supports and Supported Catalysts: Theoretical and Applied Concepts*, Butterworth-Heinemann, 1987.
2. Wu, X., Zhang, L., Weng, D., et al., *J. Hazard. Mater.*, 2012, vols. 225–226, p. 146.

3. Yoshida, H., Yazawa, Y., and Hattori, T., *Catal. Today*, 2003, vol. 87, p. 19.
4. Yazawa, Y., Takagi, N., Yoshida, H., et al., *Appl. Catal., A*, 2002, vol. 233, p. 103.
5. Ozawa, M. and Araki, K., *Surf. Coat. Technol.*, 2015, vol. 271, p. 80.
6. Chen, D., Zhang, L.H., Li, H.Z., and Liu, Y., *Appl. Surf. Sci.*, 2014, vol. 301, p. 280.
7. Checmanowski, J.G. and Szczygieł, B., *Corros. Sci.*, 2008, vol. 50, p. 3581.
8. Yin, F., Ji, S., Zhao, F., Zhou, Z., and Li, C., in *Proc. 8th Natural Gas Conversion Symp.* (Natal, Brazil, 2007), Amsterdam: Elsevier, 2007, p. 1.
9. Zhao, L., Ji, S., Yin, F., Lu, Z., Liu, H., and Li, C., *J. Nat. Gas Chem.*, 2006, vol. 15, no. 4, p. 287.
10. Powder Diffraction File database, International Center for Diffraction Data. <http://www.icdd.com/products/pdf4.htm>.
11. Inorganic Crystal Structure Database, Fachinformationszentrum Karlsruhe. [http://www2.fiz-karlsruhe.de/icsd\\_home.html](http://www2.fiz-karlsruhe.de/icsd_home.html).
12. Lippens, B.C. and Steggerda, J.J., in *Physical and Chemical Aspects of Adsorbents and Catalysts*, Linsen, B.G., Ed., Academic Press, 1970.
13. Zhou, R.-S. and Snyder, R.L., *Acta Crystallogr.*, 1991, vol. 47, p. 617.
14. *Spravochnik khimika* (Handbook for Chemists), Nikol'skii, B.P., Ed., Moscow, Leningrad: Khimiya, 1982, vol. 1, p. 382.

Translated by R.A. Safiullin